

Exotic Superfluid States of Lattice Fermions in Elongated Traps

D.-H. Kim,¹ J. J. Kinnunen,¹ J.-P. Martikainen,² and P. Törmä¹

¹*Department of Applied Physics, P.O. Box 15100, 00076 Aalto University, Finland*

²*NORDITA, 106 91 Stockholm, Sweden*

(Dated: November 11, 2019)

The nature of pairing of fermions with spin polarization is a fundamental problem in many areas of physics, including superconductors in a strong magnetic field, neutron-proton pairing in nuclear matter, and color superconductivity in high density QCD [1–3]. Non-BCS pairing mechanisms have been proposed for spin-polarized fermions. The Fulde-Ferrell-Larkin-Ovchinnikov (FFLO) states exhibit pairing with finite momentum [4, 5]. The polarized superfluid states, so-called Sarma or breached-pair states, are another candidate [6–10]. In ultracold Fermi gases [11, 12], recent experiments characterized the critical polarization of the transition to the normal state and the phase separation of the trapped gases into superfluid and normal parts [13–16]. Here we present real-space dynamical mean-field theory calculations for attractively interacting fermions in lattices with elongated traps. The critical polarization is found to be 0.8, regardless of the trap elongation. Below the critical polarization, we find unconventional superfluid structures where the polarized superfluid and Fulde-Ferrell-Larkin-Ovchinnikov-type states emerge across the entire core region.

The realization of ultracold atomic Fermi gases opens exciting opportunities for studying challenging quantum many-body problems in a highly controllable environment. In particular, here we focus on the superfluidity of spin-polarized Fermi gases. With atomic ^6Li gases, the population imbalance between the two spin components has been recently realized in elongated traps [13–17]. This system provides a new access to the interplay between fermionic superfluidity and spin polarization. Especially, it allows unprecedented access to explore the existence of stable exotic superfluid states. The Fulde-Ferrell-Larkin-Ovchinnikov (FFLO) states exhibit pairing with finite momentum, causing spatially oscillating pair potentials [4, 5]. In the polarized superfluid states, pairing with zero momentum occurs, allowing excess unpaired particles [6–10].

The FFLO and polarized superfluid states have been originally proposed for translationally invariant systems. The FFLO state, in particular, has been suggested to be stabilized by reduced dimensionality. Therefore it is important to consider systems with broken translational symmetry, especially since the ultracold gases are essentially confined in a trap, which is often highly elongated in experiments. In previous mean-field theory calculations with explicit trap confinement, the FFLO-type os-

cillations have been expected to occur only at the narrow edges the superfluid core [18]. Apart from the system geometry, another crucial issue is the role of quantum fluctuations. Most studies of the FFLO and polarized superfluid states have been based on mean field theory. Beyond mean field descriptions exist only for 1D or translationally invariant (local density approximation (LDA)) systems. Our study is the first one to explicitly describe both a realistic 3D trapping geometry and full local quantum fluctuations via dynamical mean field theory.

We study the problem of a trapped lattice fermion system at zero temperature ($T = 0$) within a *real-space* dynamical mean-field theory (DMFT) [19–22]. We solve the attractive Hubbard model with on-site interaction and an anisotropic trapping potential (see Methods section for details). The real-space DMFT explicitly considers the effect of trapping potentials with self-consistently describing site-dependent quantum fluctuations. With various trap aspect ratios examined for elongated traps, we find the critical polarization near 0.8 insensitive to the trap aspect ratios. In a wide range of polarizations, we observe that polarization and finite pair potential coexist at the core region, indicating the polarized superfluid core, surrounded by the normal unpaired particles. In highly elongated traps, as we approach the critical polarization, we find that the FFLO-type states emerge with spatially oscillating pair potential across the trap center. For comparison, we present also mean field calculations based on the Bogoliubov-de Gennes approach.

Figure 1 shows how the distribution of particles and their superfluid characteristics change with polarization P in an elongated trap with an aspect ratio $\alpha = 7.5$. The density difference $\delta n_i \equiv n_{i\uparrow} - n_{i\downarrow}$ and the pair potential $\Delta_i \equiv \langle c_{i\uparrow}^\dagger c_{i\downarrow}^\dagger \rangle$ are shown for the sites in the $y = 0$ plane. For small polarizations, the paired particles at the trap center are clearly distinguished from the unpaired particles in the surroundings as indicated by the dark central area with vanishing δn . For these small P 's, the oscillations in Δ can be found at the intermediate regions along the axial (z) direction, which can be interpreted as an analog of the proximity effect at a superconductor-ferromagnet interface [23].

As P increases, the central suppression of δn becomes weaker, and the superfluid core with finite Δ shrinks correspondingly. At $P = 0.8$, we find that Δ is completely suppressed, indicating a transition to the normal phase. At the polarizations $P \gtrsim 0.7$, we also observe the oscillatory structures in Δ emerging across the trap center, which indicates that FFLO-type states exist at high P 's

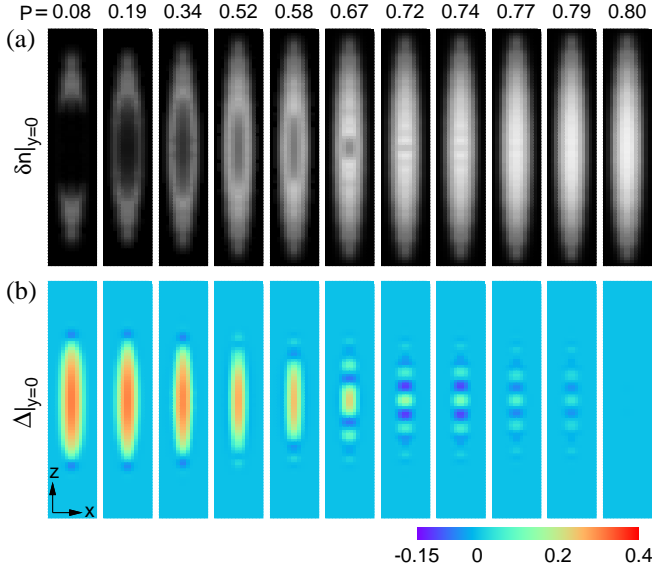


FIG. 1: Cross-sectional visualization of the particle distribution and pair potential structure in the elongated trap with the aspect ratio $\alpha = 7.5$ for selected polarizations $P \leq 0.8$. (a) The density difference $\delta n \equiv n_{\uparrow} - n_{\downarrow}$ is plotted in the $y = 0$ plane. The brighter (darker) gray indicates the larger (smaller) value of δn . Black defines $\delta n = 0$. (b) The pair potential $\Delta(x, y = 0, z)$ shows the evolution of the superfluid core structure as a function of P . The FFLO-like oscillations are observed at high P 's but below $P = 0.8$ at which Δ starts to be completely suppressed.

in this elongated system.

It turns out that the critical polarization $P_c \sim 0.8$ is insensitive to the trap aspect ratios that we have examined, and the value agrees with $P_c \sim 0.78$ found in the experiments in Refs. [15] and [16]. Figure 2(a) shows the order parameter averaged over the whole system, $\sum_i |\Delta_i|^2 / N_{\downarrow}$. All data with different trap aspect ratios follow the same trend, indicating the complete suppression of pair potentials throughout the system at $P \sim 0.8$. The behavior of our order parameter is consistent to the condensate fraction experimentally measured in Ref. [15].

On the other hand, we find that pairing in the superfluid core in our systems is unconventional. Figure 2(b) indicates the coexistence of nonzero density difference δn and large pair potential Δ at center. This polarized superfluid core is apparent at intermediate or even at low polarizations with large aspect ratios. The development of the finite δn at center seems to be a smooth function of the total polarization P . The central density difference δn depends clearly on the aspect ratio while the order parameter is nearly independent on it. Note that the role of finite size effects in our computations cannot be excluded. The features that we have found here remain unchanged for different total number of particles within the range $N = 190 - 220$.

Now let us discuss in greater detail how the cloud structure and the superfluid pairing evolve with the polarization. Figure 3 presents the axial density profiles of the

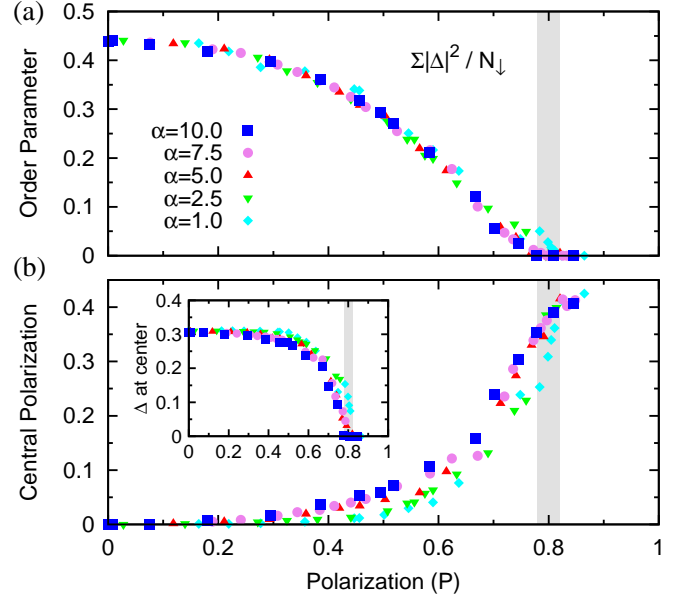


FIG. 2: Transition to the normal phase with increasing polarization P examined for various trap aspect ratios α . (a) Overall superfluid order parameter $\sum_i |\Delta_i|^2 / N_{\downarrow}$ vanishes above $P_c \sim 0.8$, regardless of α . (b) Central polarization $(n_{\uparrow} - n_{\downarrow}) / (n_{\uparrow} + n_{\downarrow})$ of the site at the cloud center becomes finite far below P_c , implying the presence of a polarized superfluid core with both finite δn and finite Δ as indicated in the inset.

majority n_{\uparrow} and minority n_{\downarrow} components, their difference δn and the pair potentials Δ along the z -axis. The calculation with $\alpha = 7.5$ is shown here as a representative example. The fully polarized majority component with $\Delta = 0$ at the edges is well separated from the superfluid core, while the core region shows nonuniform pair potentials that change with the polarization.

At very low polarization $P = 0.08$, the two components are fully paired in the central region, and small oscillations in Δ appear in the narrow intermediate regions. As P increases, n_{\uparrow} and n_{\downarrow} start to deviate from each other in the central region, leading to the wide dip area with finite δn as shown in the panels for $P = 0.31, 0.58, 0.67$ in Fig. 3. These dip regions with finite δn are also associated with a finite and non-oscillatory value of Δ , which characterizes the polarized superfluidity. The dip region gets narrower with increasing P while the intermediate region with the oscillations in Δ gets wider.

When P increases further, the dip in δn finally disappears, and the FFLO-type oscillations in Δ spread across the trap center, as plotted for $P = 0.74$ in Fig. 3. As P approaches the critical polarization, the oscillation amplitude becomes smaller and finally vanishes near $P = 0.8$. Along with the oscillations in Δ , we also find the corresponding oscillations in δn as expected in the FFLO phase. The δn oscillations have a half period of the Δ oscillations, which is consistent with the previous predictions of the FFLO-type phase in the exact numerics in

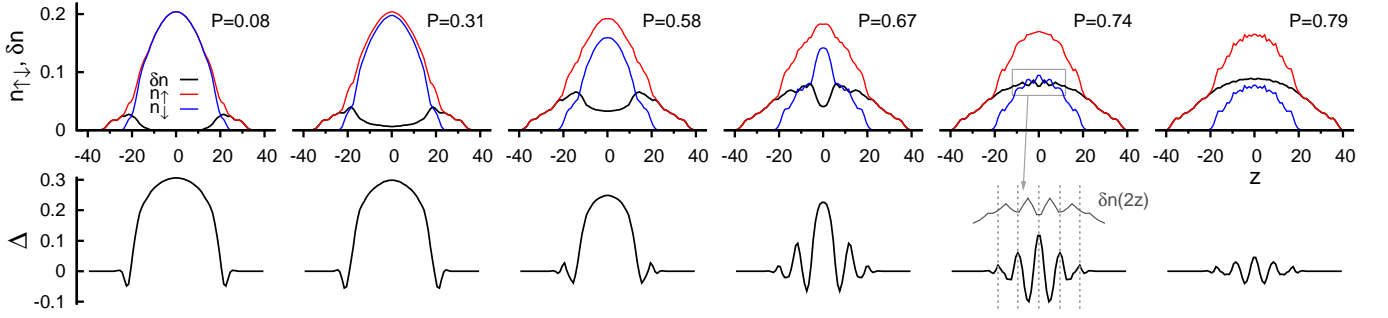


FIG. 3: Evolution of the cloud structure with increasing polarization P . Axial density profiles n and pair potential Δ are shown along the z -axis. The plots are selected for the trap aspect ratio $\alpha = 7.5$. The coexistence of the finite dip in the density difference $\delta n \equiv n_{\uparrow} - n_{\downarrow}$ and a finite Δ at the central region characterizes the polarized superfluid core. The central dip in δn disappears at high $P = 0.74$, replaced by the FFLO-type oscillations in $\Delta(z)$ spreading across the trap center.

one dimensional systems [24].

We find that these FFLO-type oscillations emerging across the trap center, rather than residing just at the edges, are found only in highly elongated traps with the trap aspect ratios $\alpha \geq 5.0$ among the examined values of α 's. The dependence of the core phase on the trap aspect ratio is summarized in Fig. 4. For $\alpha = 1.0$ and 2.5, we have found the oscillations of Δ reside only at the edges for all $P < P_c$.

The diagram in Fig. 4 separates the phases of the central region of the traps into fully paired superfluid (SF), polarized superfluid (pSF), FFLO, and normal (N). In highly elongated traps, the FFLO-type phase can be signaled by the disappearance of the central dip in δn , as shown in Fig. 3. The boundary between SF and pSF is rather unclear because δn becomes finite gradually with increasing P . However, our calculations show a tendency for the central polarization to grow faster as the trap gets more elongated.

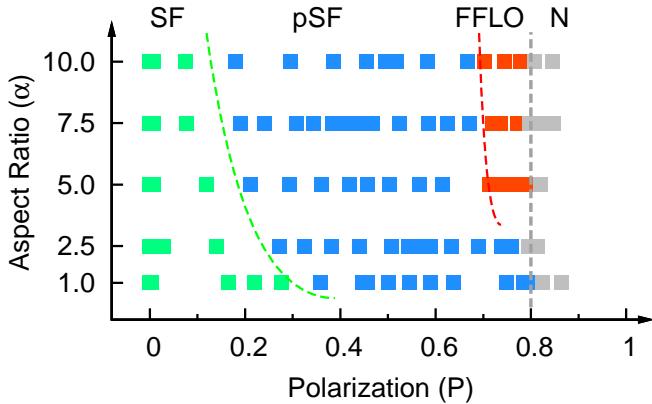


FIG. 4: Trap aspect ratio α and polarization P dependence of the phase of the central region of the trap. Fully paired superfluid (SF) is found at low P 's and continuously evolves into the polarized superfluid (pSF). The pSF is specified with the central polarization larger than 0.005. At higher P 's, the FFLO-type phase are identified for $\alpha \geq 5.0$. The dashed lines between the phases are drawn for guidance.

The nature of the polarized superfluidity found in our real-space DMFT calculations at $T = 0$ can be very subtle. It has not been clear yet how stable pSF is at $T = 0$, especially in a trap. The breached-pair state is in general energetically unstable toward the phase separation at a weak coupling at $T = 0$ [25, 26]. For a strong coupling, an earlier DMFT calculation in half-filled homogeneous cubic lattices found that the pSF may be stable down to a very low temperature [27], while other calculations suggested that the density difference may decay exponentially with decreasing temperature in quarter-filled infinite dimensional lattices [28]. In our benchmark calculations for *homogeneous* lattices (single site impurity problem, no FFLO possible) at $T = 0$, we have observed a sharp SF-N transition, as $\mu_{\uparrow} - \mu_{\downarrow}$ increases, without the intermediate pSF phase. The stability issue can be more complex in our trapped asymmetric systems. In our calculations, we have observed nonstandard (pSF)-FFLO-N type structures in the elongated traps, which cannot be explained in terms of the LDA assuming locally homogeneous systems.

Our real-space DMFT inspires the question how different are the results qualitatively from those given by the Bogoliubov de-Gennes (BdG) mean-field theory. The DMFT is based on a discrete lattice system, nevertheless we choose to compare to a BdG approach without a lattice (the density of our lattice fermions is well below the quarter filling). The BdG approach is a *static* mean-field theory widely used to incorporate a trapping potential explicitly (see Methods section). Figure 5 shows our solution of the BdG equations at unitarity in the elongated trap with the aspect ratio $\alpha = 10$. In the BdG solutions, the critical polarization is found very high, at $P \sim 0.95$, and we observe the strong deformation of the core shape at high P 's. These features are in clear contrast with those found in our real-space DMFT. The DMFT accurately describes local quantum fluctuations that are missing in the BdG theory. Such effects may cause the large deviation in the critical polarization in the strongly interacting regime.

In conclusion, using the real-space DMFT at zero temperature, we have calculated the critical polarization

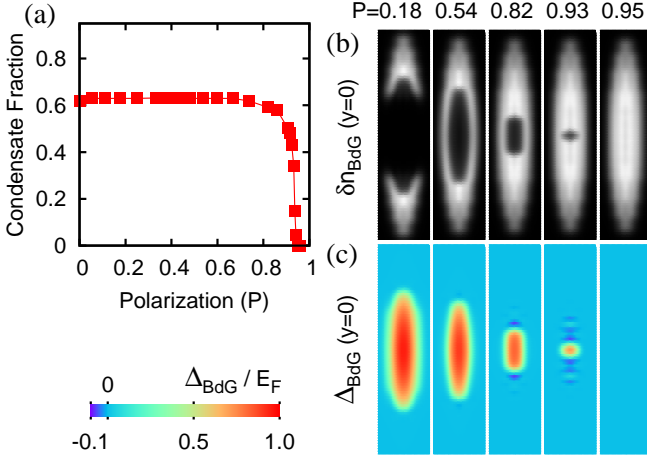


FIG. 5: BdG calculations at unitarity in the elongated trap with $\alpha = 10$ are presented for comparison. (a) The condensate fraction is plotted as a function of the polarization P . (b) The density difference δn_{BdG} and (c) the pair potential Δ_{BdG} in the $y = 0$ plane are also shown for selected polarizations. The pair potential is normalized by the Fermi energy E_F . The majority component N_\uparrow is fixed at 200 for a given P .

and found out evidence of exotic superfluid phases of polarized lattice fermions in elongated traps. Despite the difference between dilute gases and low-filling lattice fermions considered here, the critical polarization $P_c \sim 0.8$ that we have found out agrees well with the experiments [15, 16]. Also, the complex structures of the superfluid cores that we have found suggest that the unconventional pairing mechanisms in the FFLO phase and the polarized superfluid phase are enhanced by the trap geometry and may be experimentally realized at a low temperature.

Methods

Our real-space DMFT solves the Hubbard model with an *anisotropic* trapping potential at zero temperature,

$$\mathcal{H} = -t \sum_{\langle ij \rangle \sigma} c_{i\sigma}^\dagger c_{j\sigma} - U \sum_i n_{i\uparrow} n_{i\downarrow} + \sum_{i\sigma} (V_i - \mu_\sigma) n_{i\sigma},$$

where $c_{i\sigma}^\dagger$ ($c_{i\sigma}$) creates (annihilates) a fermion with spin σ at site i , the density operator $n_{i\sigma} = c_{i\sigma}^\dagger c_{i\sigma}$, and μ_σ denotes the spin-dependent chemical potential. The hopping strength t between neighboring sites $\langle ij \rangle$ is set to be unity. The attractive interaction U is chosen as the unitarity value for the cubic lattice, $U \simeq 7.915$ [29]. The anisotropic harmonic trapping potential is given as $V_i = V_0[x'^2 + y'^2 + (z'/\alpha)^2]$ where V_0 and α are the har-

monic trapping potential strength and trap aspect ratio. The coordinates of site i are assigned as $\xi' = \xi - 1/2$, where $\xi \in \{x, y, z\}$, and $\xi = -L_\xi/2, \dots, L_\xi/2 - 1$ in the three-dimensional lattice with size $L_x \times L_y \times L_z$.

The real-space DMFT is constructed for inhomogeneous systems by considering local, yet site-dependent, self-energy terms, which explicitly include trap effects beyond the local density approximation (LDA). Accordingly, the impurity problem inherent in DMFT also becomes site-dependent and must be solved for each site, which requires an efficient and fast solver. Here we employ the exact diagonalization (ED) method to solve a 7-orbital impurity Hamiltonian with a superconducting bath [19]. There are two advantages in choosing the ED method. First, as the ED method is flexible, it is straightforward to consider the generalized Anderson model with a superconducting bath which is required to describe the superfluid phases. Second, it efficiently finds the ground state which we are after at zero temperature. The possible source of error is the effective bath that consists of a limited number of orbitals, causing spiky spectral functions.

We consider harmonic trapping potentials with five different trap aspect ratios $\alpha = 1, 2.5, 5, 7.5, 10$. The chemical potentials are adjusted to fix the total particle number $N = N_\uparrow + N_\downarrow \sim 210$ with the polarization $P = (N_\uparrow - N_\downarrow)/N$. The particle density is below quarter filling at all lattice sites. The trap potential strength V_0 is chosen as 0.02 at $\alpha = 1$ and scales with $\alpha^{2/3}$ to keep the volume constant. The size of the lattice varies accordingly with α : $(L_x, L_y, L_z) = (24, 24, 24)$ for $\alpha = 1$, $(16, 16, 40)$ for $\alpha = 2.5$, $(14, 14, 70)$ for $\alpha = 5$, $(14, 14, 80)$ for $\alpha = 7.5$, and $(14, 14, 100)$ for $\alpha = 10$.

The Bogoliubov-de Gennes (BdG) mean-field method and the calculation of the condensate fraction are described in Ref. [30]. The BdG method therein for a spherical symmetric trapping potential is generalized here for describing an elongated trap by incorporating the cylindrical symmetry of the asymmetrical harmonic potential into the calculations. The reduced symmetry increases the computational load, limiting our calculations to at most 10^3 atoms at unitarity.

Acknowledgements

This work was supported by the Academy of Finland (Projects No. 213362, No. 217043, No. 217045, No. 210953, and No. 135000) and EuroQUAM/FerMix, and conducted as a part of a EURYI scheme grant (see www.esf.org/euryi). Computing resources were provided by CSC – the Finnish IT Centre for Science and the Triton cluster at the Aalto University.

[1] Casalbuoni R. & Nardulli, G. Inhomogeneous superconductivity in condensed matter and QCD. *Rev. Mod. Phys.* **76**, 263–320 (2004).

[2] Radovan, H. *et al.* Magnetic enhancement of superconductivity from electron spin domains. *Nature* **425**, 51–55 (2003).

- [3] Kenzelmann, M. *et al.* Coupled superconducting and magnetic order in CeCoIn₅. *Science* **321**, 1652–1654 (2008).
- [4] Fulde, P & Ferrell, R. A. Superconductivity in a strong spin-exchange field. *Phys. Rev.* **135**, A550–A563 (1964).
- [5] Larkin, A. I. & Ovchinnikov, Y. N. Nonuniform state of superconductors. *Zh. Eksp. Teor. Fiz.* **47**, 1136–1146 (1964) [*Sov. Phys. JETP* **20**, 762 (1965)].
- [6] Sarma, G. On the influence of a uniform exchange field acting on the spins of the conduction electrons in a superconductor. *J. Phys. Chem. Solids* **24**, 1029–1032 (1963).
- [7] Liu, W. V. & Wilczek, F. Interior gap superfluidity. *Phys. Rev. Lett.* **90**, 047002 (2003).
- [8] Sheehy, D. E. & Radzihovsky, L. BEC-BCS crossover in “magnetized” feshbach-resonantly paired superfluids. *Phys. Rev. Lett.* **96**, 060401 (2006).
- [9] Parish, M. M. Baur, S. K. Mueller, E. J. & Huse, D. A. Quasi-one-dimensional polarized Fermi superfluids. *Phys. Rev. Lett.* **99**, 250403 (2007).
- [10] Pilati, S. & Giorgini, S. Phase separation in a polarized Fermi gas at zero temperature. *Phys. Rev. Lett.* **100**, 030401(2008).
- [11] Bloch, I. Dalibard, J. & Zwerger, W. Many-body physics with ultracold gases. *Rev. Mod. Phys.* **80**, 885–964 (2008).
- [12] Giorgini, S. Pitaevskii, L. P. & Stringari, S. Theory of ultracold atomic Fermi gases. *Rev. Mod. Phys.* **80**, 1215–1274 (2008).
- [13] Zwierlein, M. W. Schirotzek, A. Schunck, C. H. & Ketterle, W. Fermionic superfluidity with imbalanced spin populations. *Science* **311**, 492–496 (2006).
- [14] Partridge, G. B. Li, W. Kamar, R. I. Liao, Y. & Hulet R. G. Pairing and phase separation in a polarized Fermi gas. *Science* **311**, 503–505 (2006).
- [15] Shin, Y. Zwierlein, M. W. Schunck, C. H. Schirotzek, A. & Ketterle W. Observation of phase separation in a strongly interacting imbalanced Fermi gas. *Phys. Rev. Lett.* **97**, 030401 (2006).
- [16] Nascimbène, S. *et al.* Collective oscillations of an imbalanced fermi gas: axial compression modes and polaron effective mass. *Phys. Rev. Lett.* **103**, 170402 (2009).
- [17] Liao, Y. *et al.* Spin-imbalance in a one-dimensional fermi gas. Preprint at <http://arxiv.org/abs/0912.0092> (2010).
- [18] Kinnunen, J. Jensen, L. M. & Törmä, P. Strongly interacting Fermi gases with density imbalance. *Phys. Rev. Lett.* **96**, 110403 (2006).
- [19] Georges, A. Kotliar, G. Krauth, W. & Rozenberg, M. J. Dynamical mean-field theory of strongly correlated fermion systems and the limit of infinite dimensions. *Rev. Mod. Phys.* **63**, 13–125 (1996).
- [20] Helmes, R. W. Costi, T. A. & Rosch, A. Mott transition of fermionic atoms in a three-dimensional optical trap. *Phys. Rev. Lett.* **100**, 056403 (2008).
- [21] Snoek, M. Titvinidze, I. Töke, C. Byczuk, K. & Hofstetter, W. Antiferromagnetic order of strongly interacting fermions in a trap: real-space dynamical mean-field analysis. *New J. Phys.* **10**, 093008 (2008).
- [22] Koga, A. Bauer, J. Werner, P. & Pruschke, T. Polarized superfluid state in a three-dimensional fermionic optical lattice. Preprint at <http://arxiv.org/abs/1006.4965> (2010).
- [23] Buzdin, A. I. Proximity effects in superconductor-ferromagnet heterostructures. *Rev. Mod. Phys.* **77**, 935–976 (2005).
- [24] Tezuka, M. & Ueda, M. Density-matrix renormalization group study of trapped imbalanced Fermi condensates. *Phys. Rev. Lett.* **100**, 110403 (2008).
- [25] Bedaque, P. F. Caldas, H. & Rupak, G. Phase separation in asymmetrical fermion superfluids. *Phys. Rev. Lett.* **91**, 247002 (2003).
- [26] Koponen, T. K. Paananen, T. Martikainen, J.-P. & Törmä, P. Finite-temperature phase diagram of a polarized Fermi gas in an optical lattice. *Phys. Rev. Lett.* **99**, 120403 (2007).
- [27] Dao, T. L. Ferrero, M. Georges, A. Capone, M. & Parcollet, O. Polarized superfluidity in the attractive Hubbard model with population imbalance. *Phys. Rev. Lett.* **101**, 236405 (2008).
- [28] Koga, A. & Werner, P. Polarized superfluidity in the imbalanced attractive Hubbard model. *J. Phys. Soc. Jpn.* **79**, 064401 (2010).
- [29] Burovski, E. Prokof’ev, N. Svistunov, B. & Troyer, M. Critical temperature and thermodynamics of attractive fermions at unitarity. *Phys. Rev. Lett.* **96**, 160402 (2006).
- [30] Jensen, L. M. Kinnunen, J. & Törmä, P. Non-BCS superfluidity in trapped ultracold Fermi gases. *Phys. Rev. A* **76**, 033620 (2007).